Summary

Adapting to a warmer climate represents a challenge for long-lived organisms such as trees. Climate also fluctuates from year to year, with consequences for adaptive dynamics. Quantitative genetics models have been developed to predict those dynamics, focusing on quantitative traits with optimal values. The impact of climate change with fluctuations on long-lived species has not been investigated yet. We model a stage-structured tree population with two stages: mature and immature individuals, each class having an optimal bud-burst date influencing respectively their fecundity and survival. Optimal dates vary from year to year and advance as climate warms. Fluctuations decrease survival, but the age structure of our population buffers the effect of fluctuating climate on the genetic composition of the population. From simulations of a process-based model of tree phenology and life cycle, we estimated a trend of advance of optimal bud-burst date of -0.15 day per year during the next century, we also showed a increase frequency of extreme events where all fecundities are equal to 0.

Introduction

Scientific consensus has been reached about the rapid environmental change we are experiencing, a rise in temperature of more than 0.8°C in the 1901-2012 period (Stocker et al., 2013). But high inter-annual variability of climate makes temperatures fluctuate around the increasing trend.

The increase of temperature caused several organisms to advance in their phenology, i.e. the timing of major events in their life cycle. There is evidence of trend to precocity in plants in their flowering time and bud-burst date (Alberto et al., 2011; Gienapp et al., 2013). Natural populations have three ways to react to environmental changes: extinction, genetic adaptation (including plasticity) or migration.

Long-lived plant species experience selection differently from annual plants because of their particular stage structure: in particular seedlings and grown trees may not experience the same selection pressures, especially under a warmer climate (Lande, 1982; Coulson and Tuljapurkar, 2008; Barfield et al., 2011; Engen et al., 2011).

Quantitative genetics models have investigated for several decades how species would react to changes in their environment (reviewed in Bürger and Krall 2004). They can predict the evolution of phenotype in populations by modeling reproduction and selection processes. Studied traits are often modeled as follow: in a given environment there is an optimal trait value, population then converge to this value to maximize fitness if achievable (Lande, 1982). To mimic variable environments they either vary the optimum in a linear fashion or randomly fluctuate it around a given mean (Lande and Shannon, 1996).

There has been an active development of models for age-structured population, but theoretical results on stage-structured population are more recent (Barfield et al., 2011). Most environmental changes model have been studied either with a trend in the evolution of the environment or with random fluctuations around a mean, but trend with fluctuations have been overlooked in the literature.

Here we focused on the effect of fluctuations on a stage-structured tree population, with bud-burst date as the evolving trait and two different optima — one for each stage. We used a previously developed demographic and quantitative genetics models (see Materials and Methods), and implemented environmental fluctuations, neglecting phenotypic plasticity. Using a process-based model describing the phenology and life cycle of Oak trees we estimated those fluctuations in optimal trait values.

Materials and Methods

Population model

We used a previously developed model with stage-structure (Sandell 2014, master's thesis). We considered a population of trees split in two classes, immature (I) and mature (M). Only mature individuals reproduce. Each year, an immature individual survive with a probability s_I, mature and reproduce with a probability m. A mature individual has a probability s_M to survive. First-time reproducers have a fecundity f_1, while experienced reproducers have a fecundity f_2. Produced seeds have a probability s_0 to survive and join the pool of immature trees. The standard parameters set is given in (Table 1). The population dynamics can be predicted using the following matrix (Caswell, 2001):

$$A = \begin{pmatrix} a_{II} & a_{IM} \\ a_{MI} & a_{MM} \end{pmatrix} = \begin{pmatrix} s_0 m f_1 + s_I(1-m) & s_0 f_2 \\ s_M m & s_M \end{pmatrix}, \tag{1}$$

where a_{ij} describes the contribution of stage j individuals to stage i the next year. With given initial conditions, we compute the number of individuals in the two stages by iterating matrix multiplication by A.

I implemented density-dependence in this model, so that the population would not continuously increase (see Figure 1). I assumed that the seed germination and survival parameter s_0 declined with increasing density of mature and immature competitors using a Beverton-Holt function (Caswell, 2001):

$$s_0 = \frac{s_{0,max}}{1 + k_I N_I + k_M N_M}, \tag{2}$$

with k_I and k_M the weights of immature (N_I) and mature (N_M) population respectively. $s_{0,max}$ is the maximum achievable s_0.

Phenotype and life-history traits

We model the evolution of a phenotypic trait, e.g. the date at which first leafs appear on a tree, z the bud-burst date. In our model, an individual is born with a given phenotype and keeps it throughout its life.

Too early bud-burst can compromise the survival of young immature trees and the fecundity of mature trees because of the risk of frost. Too late bud-burst also affects the same traits because the bad season arrives before enough photosynthetates have accumulated to guarantee survival of young trees and maturation of fruits. We assume that the survival of large mature trees is less sensitive to variation of phenology. We therefore supposed that for each individual - s_I immature survival, f_1 first reproducers and f_2 experienced reproducers fecundities (see Equation 1) to be Gaussian function of phenotype z. Thus, bud-burst date directly influences their values. They are expressed as follows:

$$\begin{cases} s_I(z) = s_I(\theta_s) \exp\left(-\dfrac{(z-\theta_s)^2}{2\omega_s}\right) \\ f_1(z) = f_1(\theta_f) \exp\left(-\dfrac{(z-\theta_f)^2}{2\omega_f}\right) \\ f_2(z) = f_2(\theta_f) \exp\left(-\dfrac{(z-\theta_f)^2}{2\omega_f}\right) \end{cases}, \tag{3}$$

θ_s is the optimal bud-burst date for survival, i.e. phenotype where s_I is at its maximum $s_I(\theta_s)$; ω_s is the width of the Gaussian function, which is inversely related to selection intensity: with small ω_s values, only a restricted range of bud-burst dates would have important survival rates (see Table 1 with standard parameters values).

The optimal trait values θ_s and θ_f can differ between stages and life-history components, but trait value does not change along the life of an individual, then there is a trade-off between fecundity and immature survival. The evolution of the trait affects the population dynamics through the life-history of the individuals in the population.

If we want to compute the mean transition rate $\overline{a_{ij}}$, we need to average s_I, f_1 and f_2 (ex: $\overline{a_{IM}} = s_0\overline{f_2}$):

$$\mathrm{E}[s_I] = \overline{s_I} = \int p_I(z)s_I(z)\,\mathrm{d}z, \tag{4}$$

with $p_I(z)$ the distribution of z in the immature stage. We suppose p_I is a Gaussian distribution with mean $\overline{z_I}$ and width P_I the phenotypic variance in the immature stage (Lande, 1982). We end with the following expression for $\overline{s_I}$:

$$\overline{s_I}(\overline{z_I}) = s_I(\theta_s)\sqrt{\frac{\omega_s}{\omega_s + P_I}}\exp\left(-\frac{(\overline{z_I} - \theta_s)^2}{2(\omega_s + P_I)}\right), \tag{5}$$

we obtain similar expressions for $\overline{f_1}$ and $\overline{f_2}$.

Iterations at each time step

Assuming the phenotype has a Gaussian distribution, the mean genotypic value of matures and immature at the next time step is given by (Barfield et al. 2011 Eq.5, applied to the current models):

$$\overline{g_I}' = (c_{IM}\overline{g_M} + c_{II}\overline{g_I}) + (c_{IM}G_M\beta_{a_{IM}} + c_{II}G_I\beta_{a_{II}}) \tag{6a}$$
$$\overline{g_M}' = (c_{MI}\overline{g_I} + c_{MM}\overline{g_M}) + (c_{MI}G_I\beta_{a_{MI}} + c_{MM}G_M\beta_{a_{MM}}), \tag{6b}$$

with $c_{ij} = \frac{n_j\overline{a_{ij}}}{n_i'}$, the contribution of stage j individuals to next years pool of stage i individuals, as a fraction of i individuals at the next time step n_i'; and $\beta_{a_{ij}}$ the selection gradient as $\beta_{a_{ij}} = \frac{\partial \ln \overline{a_{ij}}}{\partial \overline{z}}$ (Barfield et al., 2011). The selection gradient represents the force of directional selection, and together with the genetic variance for the trait (G), is used to predict the change in mean phenotype due to the response to selection (Lande, 1982).

The first term is a weighted average of mean genotypes contributing to this stage; while the second shows the effect of selection.

To have the formal expressions of $\beta_{a_{ij}}$ we need to compute the selection gradients on life-history components:

$$\begin{aligned}
\beta_{\overline{s_I}} &= \frac{\partial \ln \overline{s_I}}{\partial \overline{z_I}} &&= \frac{\theta_s - \overline{z_I}}{\omega_s + P_I} \\
\beta_{\overline{f_1}} &= \frac{\partial \ln \overline{f_1}}{\partial \overline{z_I}} &&= \frac{\theta_f - \overline{z_I}}{\omega_f + P_I} \\
\beta_{\overline{f_2}} &= \frac{\partial \ln \overline{f_2}}{\partial \overline{z_M}} &&= \frac{\theta_f - \overline{z_M}}{\omega_f + P_M}.
\end{aligned} \tag{7}$$

Because we have for example $\overline{a_{II}} = s_0 m\overline{f_1} + \overline{s_I}(1-m)$ we get the selection gradient:

$$\beta_{a_{II}} = \frac{s_0 m\overline{f_1}\beta_{\overline{f_1}} + \overline{s_I}\beta_{\overline{s_I}}(1-m)}{\overline{a_{II}}}. \tag{8}$$

We have a similar recursion for phenotypes (Barfield et al., 2011). We need to distinguish direct transitions of individuals from one stage to the other $\overline{t_{ij}}$ and events leading to new individuals $\overline{f_{ij}}$ (note

$\overline{a_{ij}} = \overline{t_{ij}} + \overline{f_{ij}}$), because in the first case the phenotype remain unchanged while in the second only the genotype is inherited:

$$\overline{z'_I} = c^t_{II}(\overline{z_I} + P_I\beta_{t_{II}}) + c^f_{II}(\overline{g_I} + G_I\beta_{f_{II}}) + c^f_{IM}(\overline{g_M} + G_M\beta_{f_{IM}}) \tag{9a}$$

$$\overline{z'_M} = c^t_{MI}(\overline{z_I} + P_I\beta_{t_{MI}}) + c^t_{MM}(\overline{z_M} + P_M\beta_{t_{MM}}), \tag{9b}$$

with $\beta_{t_{ij}}$ the gradient of selection defined as above in Equation 6a, i.e. $\beta_{t_{ij}} = \frac{\partial \ln \overline{t_{ij}}}{\partial \overline{z}}$; $c^t_{ij} = \frac{n_j \overline{t_{ij}}}{n'_i}$ the contribution by direct transition of stage j to stage i and $c^f_{ij} = \frac{n_j \overline{f_{ij}}}{n'_i}$ the contribution by birth.

Approximation under weak selection

Under weak selection, the mean phenotype at equilibrium in the population $\overline{z}$ follows in a constant environment (Engen et al., 2011):

$$\overline{z_{eq}} = \frac{\gamma_f\theta_f + \gamma_s\theta_s}{\gamma_f + \gamma_s}, \tag{10}$$

with,

$$\gamma_f = \frac{v_I u_I s_0 m \overline{f_1}}{\lambda(P_I + \omega_f)} + \frac{v_I u_M \frac{G_M}{G_I} s_0 \overline{f_2}}{\lambda(P_M + \omega_f)}, \tag{11a}$$

and

$$\gamma_s = \frac{v_I u_I \overline{s_I}(1-m)}{\lambda(P_I + \omega_s)}. \tag{11b}$$

γ_f and γ_s represent the respective weight of each of the optimum in the trade-off between θ_f and θ_s for $\overline{z_{eq}}$. Indeed, if $\theta_f = \theta_s$ then $\overline{z_{eq}} = \theta_f = \theta_s$. But if $\theta_f \neq \theta_s$, then the position of the mean phenotype depends on γ_f and γ_s.

Fluctuating optima

I introduced environmental fluctuations in the model through the optima:

$$\begin{cases} \theta_f(t) = \overline{\theta_f} + \alpha_f\xi_f(t) \\ \theta_s(t) = \overline{\theta_s} + \alpha_s\xi_s(t) \end{cases}, \tag{12}$$

α_i is the sensitivity of θ_i to noise ξ_i. ξ_f and ξ_s are noise vectors drawn at each time step from a bi-variate normal distribution with respectively σ^2_f and σ^2_s variances and correlation ρ_N.

Under varying environment we get an another approximation under weak selection from (Engen et al., 2011) describing the change of mean phenotype:

$$\Delta\overline{z}(t) = -G_I\gamma(\overline{z}(t) - \theta_v(t)), \tag{13}$$

with

$$\gamma = \gamma_f + \gamma_s, \tag{14a}$$

$$\theta_v(t) = \overline{z_{eq}} + \xi_v(t), \tag{14b}$$

$$\xi_v(t) = \frac{\alpha_f\xi_f(t) + \alpha_s\xi_s(t)}{\alpha_f + \alpha_s}. \tag{14c}$$

We see that the change in the mean phenotype depends on the sensitivity to noise of the optima α_i as well as on the magnitude of the variations.

Trend in change

To model climate-change, and especially the trend of increasing temperature with time, we included a trend in the variation of the optima:

$$\begin{cases} \theta_i(t) = \overline{\theta_i} + \alpha_i \epsilon(t) \\ \epsilon(t) = kt + \xi_i(t) \end{cases}. \tag{15}$$

With k having a negative value, the optima tend to decrease with time.

PHENOFIT simulations

PHENOFIT is a phenology model including several sub-models; from environmental and phenological data it simulates the survival and reproduction of an average tree to predict its range (Morin et al., 2008).

We used output from PHENOFIT (simulations performed by A. Duputié) from 1950 to 2100 for the sessile oak (*Quercus petraea*), namely predicted bud burst date and predicted fecundities in 6 localities (see Figure 4). We had fecundity predictions for phenotypes around the modeled date (a range of 42 days). From these data we predicted the optima fluctuations. Considering fecundity f as a Gaussian function around this date with the same form as f_1 in Equation 5:

$$\beta = \frac{\partial \ln f}{\partial \overline{f}} = \frac{\theta_f - \overline{z}}{\omega_f + \sigma_z^2}, \tag{16}$$

using (Lande and Arnold, 1983), with z Gaussian, $p(z)$ the distribution of z in the population, $f(z)$ the fitness associated with z and $\overline{f}$ the mean fitness in the population, we computed selection gradients from PHENOFIT simulation outputs as:

$$\beta = \frac{\mathrm{cov}(z, \frac{f(z)}{\overline{f}})}{\sigma_z^2}. \tag{17}$$

From (16) and (17) we can express θ_f:

$$\theta_f = \frac{\mathrm{cov}(z, \frac{f(z)}{\overline{f}})}{\sigma_z^2}(\omega_f + \sigma_z^2) + \overline{z}. \tag{18}$$

In our estimations we considered $p(z)$ to be Gaussian around the modeled date by PHENOFIT, with a variance of $P_I = 40$ as in our analytic model. We normalized this distribution so that all dates in the population would be in the 42 days interval around the modeled date.

Trend analyses

All statistical analyses were made using R (R Core Team, 2014), graphics were drawn using ggplot2 (Wickham, 2009), data were handled using dplyr (Wickham and Francois, 2014).

To estimate the trend of the θ_f variations, we considered a trend model with three components: a general decreasing linear trend, a white noise component with a constant variance and a more dramatic noise leading to "catastrophic" events, with low θ_f values.

The regular noise and the trend were estimated excluding those catastrophic events, we kept only value of θ_f over 60, which is the lower bound of the observed range of bud burst date of oak trees. Then we performed a linear regression between values of θ_f and time, giving us an estimation of k from Equation 15. Analyzing the residuals gives us the variance of $\alpha_f \xi_f$ from the same equation.

Parameter	Notation	Value
Life Cycle		
Optimal phenotype for fecundity	θ_f	100
Optimal phenotype for immature survival	θ_s	130
Fecundity function width	ω_f	400
Survival function width	ω_s	400
Heritability	h^2	0.5
Phenotypic variance of immature	P_I	40
Phenotypic variance of matures	P_M	40
Genotypic variance of immature	$G_I = P_I \times h^2$	20
Genotypic variance of matures	G_M	20
Survival of immature at phenotypic optimum	$\overline{s_I}(\overline{z} = \theta_s)$	0.8
Fecundity of first time reproducers at optimum	$\overline{f_1}(\overline{z} = \theta_f)$	100
Fecundity of experienced reproducers at optimum	$\overline{f_2}(\overline{z} = \theta_f)$	200
Maturation rate of immature	m	0.02
Combined survival and germination rate of seed	s_0	0.03
Survival of mature stage	s_M	0.99
Density-dependence		
Maximum s_0 in density-dependence function	$s_{0,max}$	0.12
Decreasing factor due to immature	k_I	0.001
Decreasing factor due to matures	k_M	0.005
Fluctuations		
Sensitivity of optimum for fecundity to fluctuation	α_f	5
Sensitivity of optimum for survival to fluctuation	α_s	5
Noise variance for fecundity	$\sigma^2_{\xi_f}$	3.725
Noise variance for survival	$\sigma^2_{\xi_s}$	3.725
Correlation between noises	ρ_N	0.5
Trend coefficient	k	-0.15

Table 1: Standard parameter set

Results

Constant environment and density-dependence

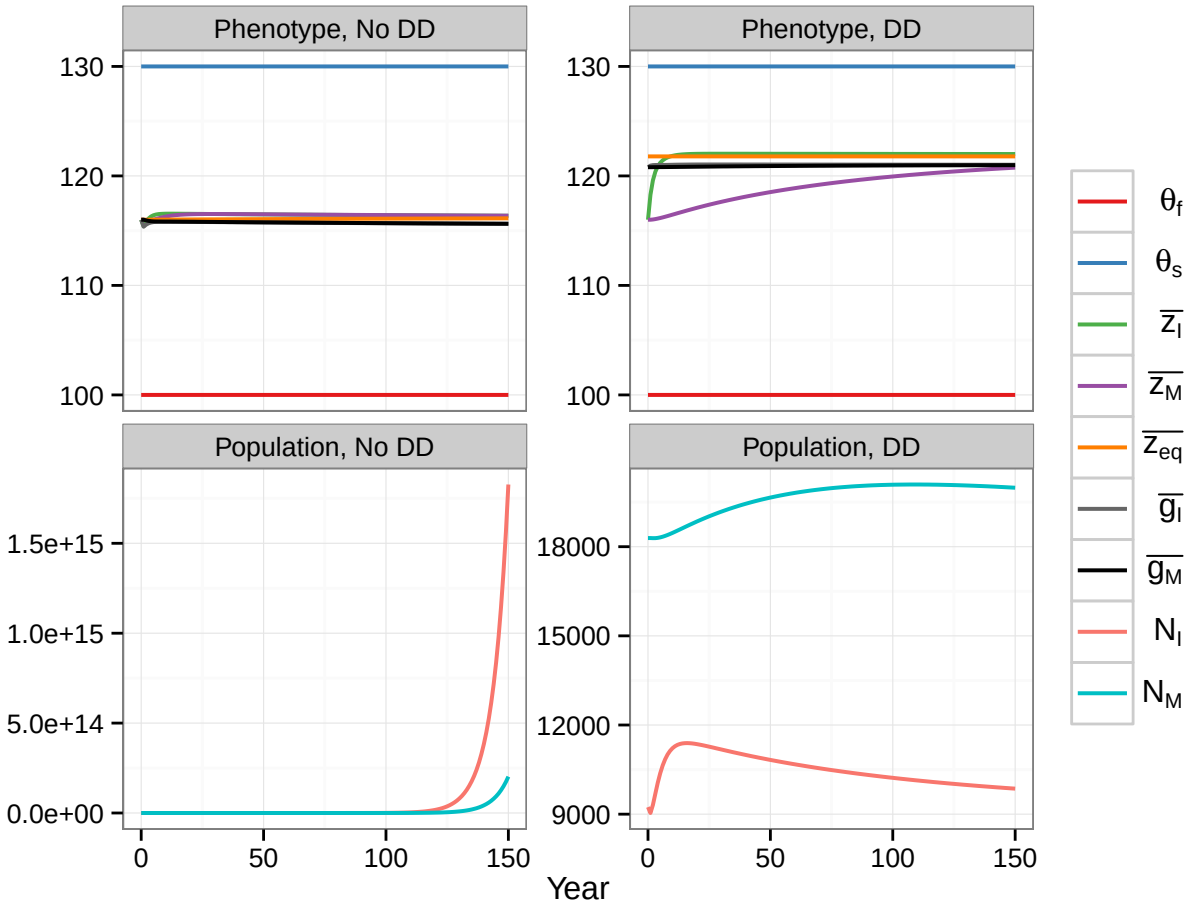

Figure 1: Effect of density-dependence on phenotypes and populations. **Top:** Phenotype variations in population ($\overline{z_I}, \overline{z_M}$, starting from $z = 116$) with their corresponding genotypic values ($\overline{g_I}, \overline{g_M}$, with $g_i(0) = 116$), and the approximation given by Equation 10; **Bottom:** Population, number of immature individuals (N_I, red), number of mature individuals (N_M, blue). Starting from the density-dependent Stable-Stage Distribution (SSD) in constant environment. **No DD** means we used the model without density-dependence, **DD** means we implemented density-dependence through s_0 (see Equation 2). Here, bud-burst date is expressed in julian days (numbered days in the year, 1st of January being 1 in julian days).

We used the previously developed model in (Sandell 2014) and simulated (see Figure 1) a tree population for 150 years in a constant environment, with and without density-dependence on s_0, to assess the effects of a more realistic demography.

As expected, density-dependence allows regulating the population (Figure 1 right panel), as the number of mature and immature individuals seem to converge respectively to 18000 and 10000 individuals, while without density-dependence the population is exponentially growing.

Looking at the phenotype, we started from exactly the same starting point $z = 116$ for phenotypic and genotypic values. Without density-dependence, the population quickly converge to the equilibrium phenotype ($\overline{z_{eq}}$ given by the approximation in Equation 10), $\overline{z_{eq}} = 116$ in this case. With density-dependence the equilibrium phenotype is shifted towards the survival optimum θ_s ($\overline{z_{eq}} = 121.8$). The lower seed survival s_0 decreases γ_f (11a) changing the weights in (10), making it more interesting to

favor the survival of already established immature trees than the production of many propagules with very little survival prospect.

The genotypic values, $\overline{g_I}$ and $\overline{g_M}$ (respectively gray and black on Figure 1) are distinct from the mean phenotype values.

The mean immature phenotype $\overline{z_I}$ converge quicker than the mean mature phenotype $\overline{z_M}$ to $\overline{z_{eq}}$. High mature trees survival in our simulations makes it long to replace them with a different genotype and phenotype. To make $\overline{z_M}$ closer to $\overline{z_{eq}}$, immature individuals with a phenotype closer to $\overline{z_{eq}}$ need to survive long enough to mature and outnumber initial mature individuals with phenotype further from $\overline{z_{eq}}$.

Fluctuating optima

To mimic a changing environment we made the optima fluctuate (Figure 2, dashed lines) and compared this model to the one in constant environment (solid lines).

The mean phenotype of the population does not change very much with the fluctuations, indeed, $\overline{z_M}$ in constant and fluctuating environment are equal, and they are also equal to $\overline{z_{eq}}$, that is why they are indistinguishable on Figure 2.

Only $\overline{z_I}$ fluctuates under varying environment, but the fluctuations have a very small variance compared to the ones of the optima. We found a stronger correlation between θ_s and $\overline{z_I}$ across years ($\rho_{\text{Pearson}} = 0.6997364$) than with θ_f. It shows how immature individuals track the variations of the survival optimum.

Because of the variations, the phenotype lags away from the optimal value,decreasing the mean of s_I in fluctuating environment. The number of immature individuals N_I is thus lower under the fluctuating regime then decreasing the number of mature individuals N_M, this decline in density in turn increases s_0. The variation in θ_s causes s_I to decrease, it reveals the cost of the fluctuations demographically: fluctuating regime causes variations in survival that may have dramatic effect on population.

However, those fluctuations do not seem to affect fecundities f_1 and f_2 in the same way (Figure 2 bottom left panel). As the mean optima move, they get closer to the population phenotype increasing fecundity, but, at the next time step, they move further away from this phenotype decreasing fecundity.

The asymmetry of responses between survival s_I and fecundities f_1 and f_2 is due to the specific trade-off occurring in our population. The mean phenotype in our simulations is closer to the mean of θ_s than to the mean of θ_f; there is a higher chance of θ_s to be lower or much higher than the mean population phenotype when it fluctuates, while θ_f can get closer to the mean population phenotype when it fluctuates.

As we had partially correlated noises in our population (see Table 1 to have standard parameters set), we varied correlations for noises between 0 and 1 in conditions affecting respectively survival and fecundity. The results were similar whatever the correlation coefficient. It seemed that the lower the correlation between noises, the higher were the demographic burden (results not shown). Uncorrelated environments decrease more the life-history traits than correlated environments.

Trend in the environment

We implemented a decreasing trend in θ_f with fluctuations (Figure 3) to mimic climate change. We simulated both a linear trend and a linear trend with fluctuations in optima variation (respectively solid and dashed lines in Figure 3).

The phenotype in the population decreases as the optima decrease, but much slower, whether with fluctuations or not. The mean phenotype in the immature stage $\overline{z_I}$ varies with the same trend with and without fluctuations, but the first still fluctuates strongly around this trend. While the mean phenotypes of mature individuals $\overline{z_M}$ are almost indistinguishable in the two types of environments,

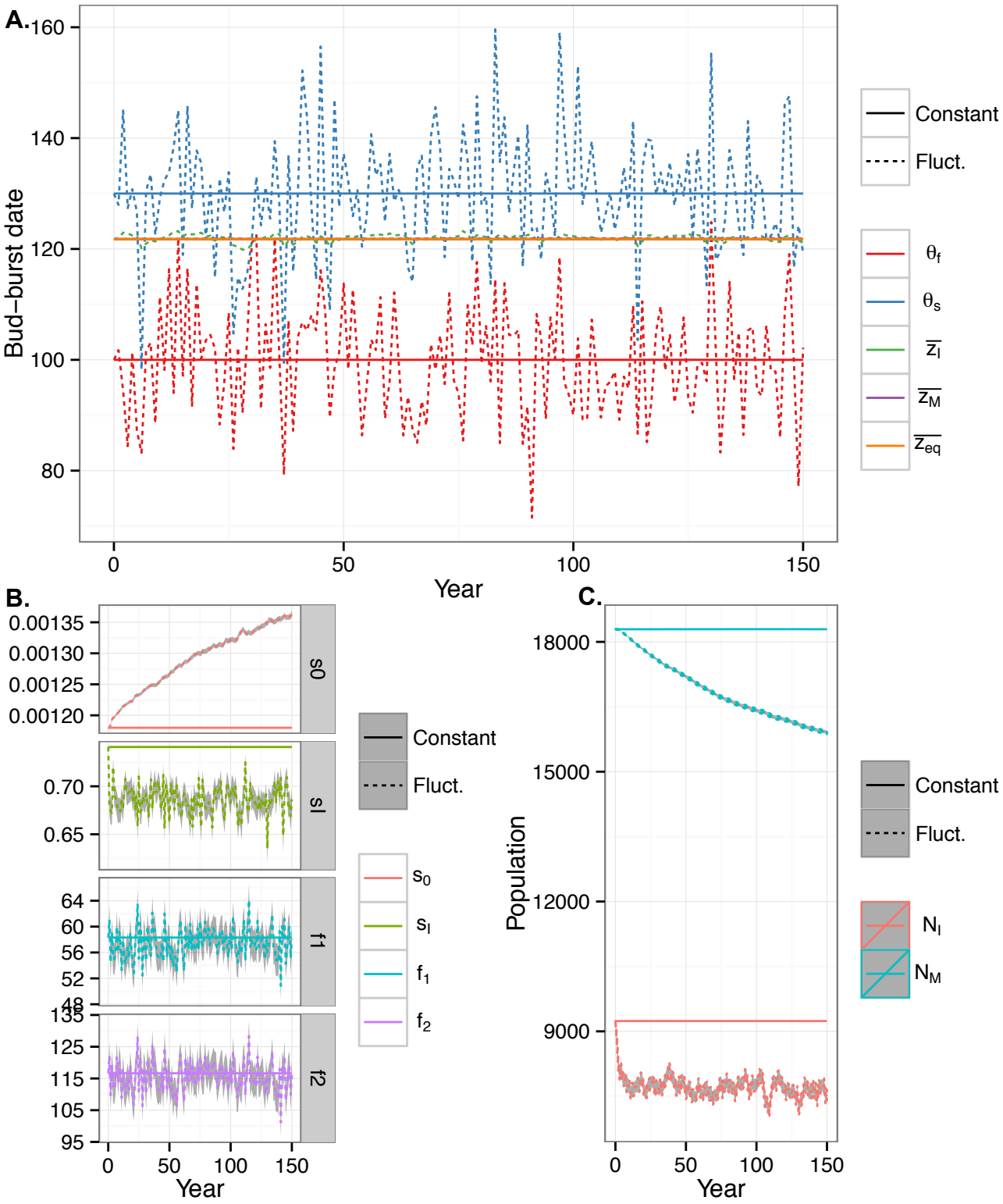

Figure 2: Fluctuating optima against constant environment. **A:** comparison of phenotypes from simulations with constant or fluctuating optima, $\overline{z_{eq}}$ is the approximation shown in Equation 10; results from single simulation. **B:** life-history traits in constant or fluctuating environment. **C:** population in constant or fluctuating environment, N_I is the number of immature individuals and N_M the number of mature individuals, population started from the stable stage distribution. **Solid lines:** values in constant environment, **Dashed lines:** in fluctuating environment, results were averaged over 100 independent simulations. **Gray envelope**: 95% confidence interval of average.

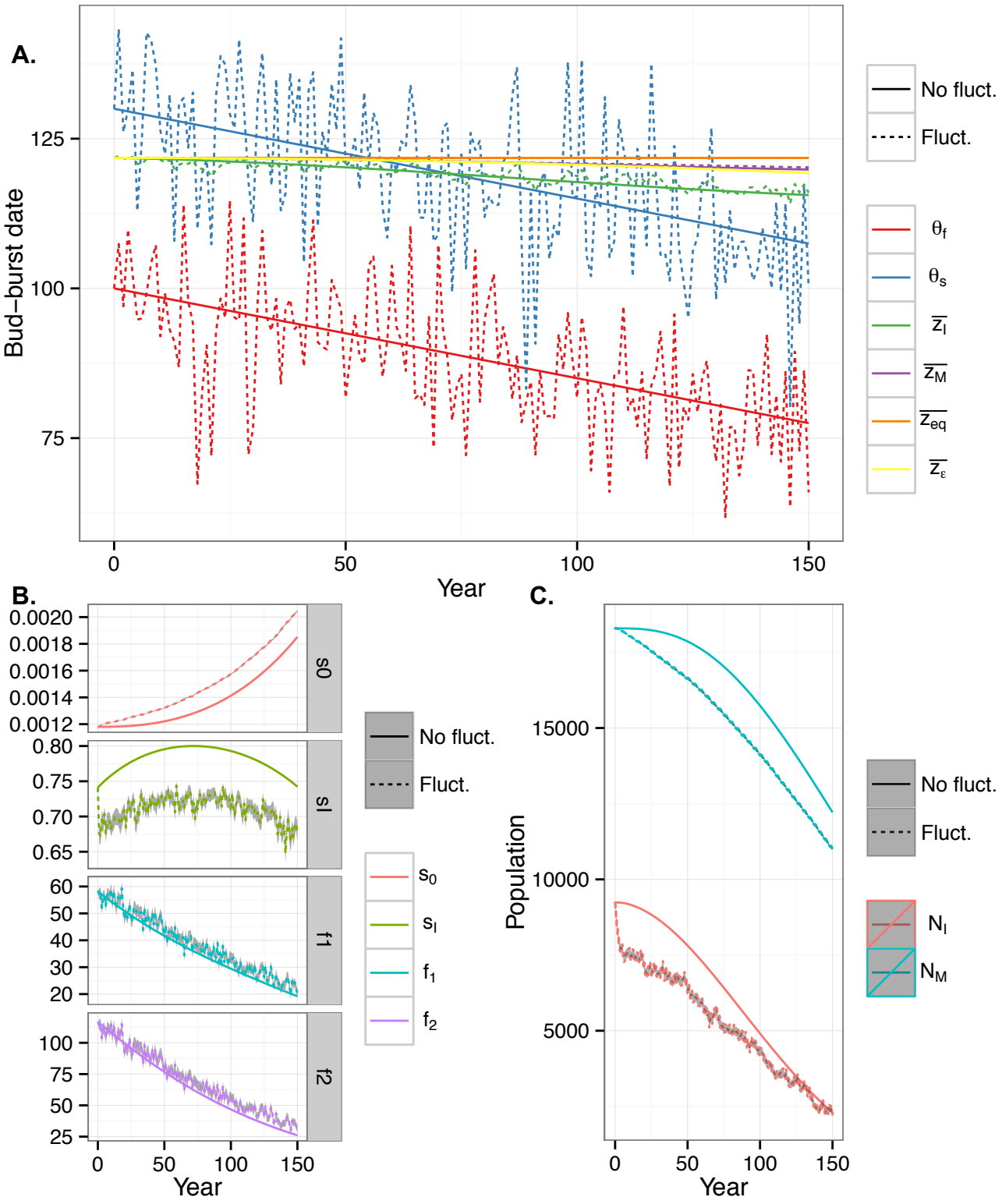

Figure 3: Mixed influences of trend and fluctuations on the population. **A:** Phenotype evolution with and without fluctuations, results from a **single** simulation; **B:** (**Left**) life-history traits evolution; **C:** demography. **Solid lines:** (**No fluct.**) linearly decreasing optima with time; **Dashed lines:** (**With fluct.**) fluctuating decreasing optima, results were averaged over 100 independent simulations. **Gray envelope**: 95% confidence interval of average.

$\overline{z_M}$ under fluctuations (dashed line) is a little bit over $\overline{z_M}$ without them (solid line). We implemented the approximation $\overline{z_\epsilon}$ from (Engen et al. 2011, see Equation 13), it follows the variations in a similar fashion as the mean phenotype of the mature individuals.

The immature survival (s_I) has an interesting behavior, it first increases, reaches a maximum, then decreases. The decreasing trend in optima variation causes at first the mean population phenotype to move closer to θ_s, thus maximizing s_I values when it crosses θ_s line, as soon as it moves beyond s_I starts to decrease again.

On the contrary f_1 and f_2 the mean population phenotype go further away from θ_f with and without fluctuation.

After a certain number of years, the population is lower in environments with trends than in constant ones, fluctuations worsen the demographic decline (Figure 3).

As expected, the decreasing trend in θ_f creates a lag between the optima and the mean population values, because adaptation is slower than the rate of change. On a very long scale (2500 years), the population however maintains itself by changing its phenotype fast enough to track the optima variation with a constant lag (data not shown).

Estimation of the fluctuations

In 6 localities (map Figure 4 bottom left) using PHENOFIT output, we computed θ_f values at these locations (top 3 rows of Figure 4). For the 6 sites, predicted θ_f decreases with time: earlier bud-burst is favored as climate warms.

Over the general trend, we observe a small amplitude variation, corresponding to year to year change in θ_f and some more episodic dramatic decreases in its values, sometimes reaching negative values (e.g. at BIC site in 1976). The frequency of these events increase with time as they become common after 2050 for all sites. Note that those events are biased towards the decrease of θ_f, as there is no equivalent dramatic increases.

The negative values of θ_f computed in Figure 4, may seem striking as negative values refer to the previous year. It indicates strong directional selection to shorten bud-burst those years. As bottom right panel of Figure 4 shows, we can have negative value of θ_f and still have achievable phenotypes. If θ_f is very negative for a given year (less than -100 in 2048 for LAB), it means there will be little reproduction this year (flat tail of blue curve, bottom right panel Figure 4).

We excluded those extreme events, taking all sites together, to estimate the trend in the variation of θ_f (see Materials and Methods). Using linear regression on θ_f with time, we found a rate of $-0.15\,\text{day.year}^{-1}$, with normal residuals having a variance of $93.125\,\text{day}^2$ (data not shown, $R^2 = 0.2341$, $p <$ 2e-16, $F = 186.7$ with 611 d.f.). From our trend model (Equation 15) we have:

$$\theta_f(t) = \overline{\theta_f} + \alpha_f k t + \alpha_f \xi_f(t). \tag{19}$$

The variance of residuals is thus:

$$\text{Var}(\alpha_f \xi_f(t)) = \alpha_f^2 \sigma_{\xi_f}^2, \tag{20}$$

which gives, with $\alpha_f = 5$, $\sigma_{\xi_f}^2 = 3.725$. Trend and variance estimations were used in previous simulations (see Table 1).

Discussion

We modeled a stage-structured tree population using a quantitative genetics approach, with bud-burst date varying between two optima. We predicted phenotype evolution in the next 150 years. Using PHENOFIT simulation results we computed values for one of the optima. According to simulations, an increasing number of extreme events will happen in the next century where all fecundities will be equal to zero.

As expected in the literature, we found a decreasing trend in the variation of optima, i.e. a trend to precocity of phenology (Aitken et al., 2008; Ehrlén and Münzbergová, 2009). Because of the general increase in temperature, organisms advance their phenology to track their original environment,

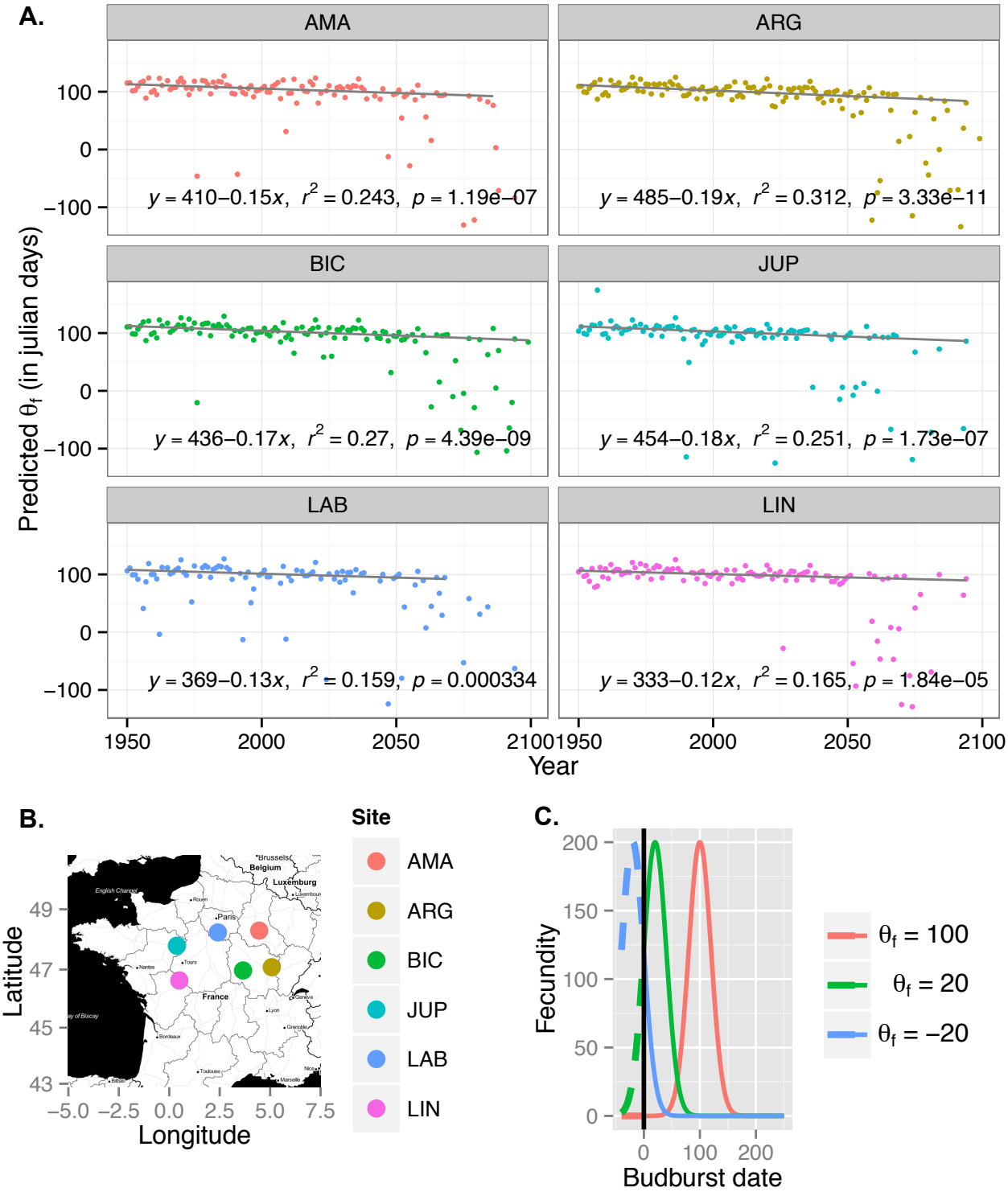

Figure 4: θ_f estimations from PHENOFIT data. **A:** estimations of θ_f for each study site (see Materials and Methods for details), linear regression only for values >60. **B:** map of the study sites. **C:** Theoretical fecundity functions with parameters from Table 1 with values of θ_f equals to 100, 20 and -20, solid lines indicate achievable phenotype, dashed lines advance towards previous year.

either by genetic change or plasticity (Savolainen et al. 2004, reviewed in Merilä and Hendry 2014). Increasing evidence underlines the role of plasticity for trees in adaptation to environmental change, we did not consider it in our model to focus on the specific effects of fluctuations on genetic adaptation as a first step in our exploration; phenotypic plasticity should also be taken into account in a future

model as it slows down genetic adaption (Alberto et al., 2013; Aitken et al., 2008).

With trend (Figure 3), counter-intuitively, there is no difference of in adaptation speed with and without fluctuations. We could have expected a cost of fluctuations for adaptation: if the population would have tracked fluctuations closely, noise fluctuations would have moved away optima from mean population phenotype for sure, decreasing fitness. As a long-lived and stage-structured species, the oak population in our model do not follow very closely those fluctuations, that is why we see no cost of fluctuations.

The mean phenotype in immature individuals $\overline{z_I}$ changes faster than the mean phenotype in mature individuals $\overline{z_M}$, there is a difference of adaptation speed between stages. The stage-structure of our population explains the different behaviors among the two classes.

Our model was parametrized according to the sessile oak life-cycle (*Quercus petraea* spp.) — using the PHENOFIT simulations to predict fluctuations and trend in the optima. The species does not go extinct in the next 150 years (Figure 3). Climate change has still dramatic demographic consequences, the population halving in less than 100 years. The sessile oak would be left more vulnerable demographically as it increases genetic drift and the potential consequences of dramatic events.

Those estimations and fluctuations did not included the extreme years when all fecundities were equal to zero, i.e. the selection gradient is zero, nor those where the optima was very negative, with very strong directional selection, those years should affect adaptation dynamics. Modeling correctly the variations of optima values would lead to more realistic behavior, it could be done by drawing the optima from an almost Gaussian distribution with a very long tail towards negative values.

Taking into account the different responses to environmental changes in various stages, more than 2 stages with their own optima could contribute in the general phenotypic equilibrium.

Those optima are of abstract nature, they are difficult to measure directly in natural populations; to overcome this difficulty, it was suggested to measure selection gradient to have access to fitness landscapes and extrapolate optima (Lynch and Lande, 1993). In the wild, a whole population do not share one single bud-burst date, they do not forcefully converge to a single optimal date; rather there exists a range of possible dates that all maximize fitness in the same way. Each individual bud-burst date may not be optimal but they converge if achievable in a range of different optimal values. Including such optimal ranges could be one step towards more realistic quantitative genetics models.

Authors Contributions and Acknowledgments

M. Grenié did the analyses and simulations, based on L. Sandell's work. O. Ronce and LM. Chevin supervised the project. A. Duputié shared PHENOFIT outputs. I. Chuine advised the project about PHENOFIT outputs.

I would like to thank Ophélie Ronce for being an extremely patient supervisor, Luis-Miguel Chevin and Isabelle Chuine for the discussions we had about the project. I thank Guillaume Martin for being an awesome office-mate. Finally, I would like to thank the whole "Metapopulations" team at ISEM for their welcome.

References

Aitken, S. N., Yeaman, S., Holliday, J. A., Wang, T. and Curtis-McLane, S. (2008). Adaptation, migration or extirpation: climate change outcomes for tree populations. Evolutionary Applications *1*, 95--111.

Alberto, F., Bouffier, L., Louvet, J.-M., Lamy, J.-B., Delzon, S. and Kremer, A. (2011). Adaptive responses for seed and leaf phenology in natural populations of sessile oak along an altitudinal gradient. Journal of Evolutionary Biology *24*, 1442--1454.

Alberto, F. J., Aitken, S. N., Alía, R., González-Martínez, S. C., Hänninen, H., Kremer, A., Lefèvre, F., Lenormand, T., Yeaman, S., Whetten, R. and Savolainen, O. (2013). Potential for evolutionary responses to climate change - evidence from tree populations. Global Change Biology *19*, 1645--1661.

Barfield, M., Holt, R. D. and Gomulkiewicz, R. (2011). Evolution in Stage-Structured Populations (2 versions). The American Naturalist *177*, 397--409.

Bürger, R. and Krall, C. (2004). Quantitative-genetic models and changing environments. Evolutionary conservation biology , 171--187.

Caswell, H. (2001). Matrix population models : construction, analysis, and interpretation. Sinauer Associates.

Coulson, T. and Tuljapurkar, S. (2008). The Dynamics of a Quantitative Trait in an Age-structured Population Living in a Variable Environment. Am Nat *172*, 599--612.

Ehrlén, J. and Münzbergová, Z. (2009). Timing of Flowering: Opposed Selection on Different Fitness Components and Trait Covariation. The American Naturalist *173*, 819--830.

Engen, S., Lande, R. and Sæther, B.-E. (2011). Evolution of a Plastic Quantitative Trait in an Age-Structured Population in a Fluctuating Environment. Evolution *65*, 2893--2906.

Gienapp, P., Lof, M., Reed, T. E., McNamara, J., Verhulst, S. and Visser, M. E. (2013). Predicting demographically sustainable rates of adaptation: can great tit breeding time keep pace with climate change? Phil. Trans. R. Soc. B *368*, 20120289.

Lande, R. (1982). A Quantitative Genetic Theory of Life History Evolution. Ecology *63*, 607--615.

Lande, R. and Arnold, S. J. (1983). The Measurement of Selection on Correlated Characters. Evolution *37*, 1210--1226.

Lande, R. and Shannon, S. (1996). The Role of Genetic Variation in Adaptation and Population Persistence in a Changing Environment. Evolution *50*, 434.

Lynch, M. and Lande, R. (1993). Evolution and extinction in response to environmental change. Biotic interactions and global change , 234--250.

Merilä, J. and Hendry, A. P. (2014). Climate change, adaptation, and phenotypic plasticity: the problem and the evidence. Evolutionary Applications *7*, 1--14.

Morin, X., Viner, D. and Chuine, I. (2008). Tree species range shifts at a continental scale: new predictive insights from a process-based model. Journal of Ecology *96*, 784--794.

R Core Team (2014). R: A Language and Environment for Statistical Computing. R Foundation for Statistical Computing Vienna, Austria.

Savolainen, O., Bokma, F., García-Gil, R., Komulainen, P. and Repo, T. (2004). Genetic variation in cessation of growth and frost hardiness and consequences for adaptation of Pinus sylvestris to climatic changes. Forest Ecology and Management *197*, 79--89.

Stocker, T. F., Qin, D., Plattner, G. K., Tignor, M., Allen, S. K., Boschung, J., Nauels, A., Xia, Y., Bex, B. and Midgley, B. M. (2013). IPCC, 2013: climate change 2013: the physical science basis. Contribution of working group I to the fifth assessment report of the intergovernmental panel on climate change. .

Wickham, H. (2009). ggplot2: elegant graphics for data analysis. Springer New York.

Wickham, H. and Francois, R. (2014). dplyr: A Grammar of Data Manipulation. R package version 0.3.0.2.